

# The Reversible Amination of Tin(II)-Ligated Imines: Latent Initiators for the Polymerization of *rac*-Lactide

Nonsee Nimitsiriwat,<sup>†</sup> Vernon C. Gibson,<sup>\*,†</sup> Edward L. Marshall,<sup>\*,†</sup> and Mark R. J. Elsegood<sup>‡</sup>

Department of Chemistry, Imperial College London, South Kensington Campus, London SW7 2AZ, U.K., and Chemistry Department, Loughborough University, Leicestershire LE11 3TU, U.K.

Received August 24, 2007

The 1:1 reactions of nine potentially tridentate salicylaldimines with tin(II) diamides,  $\text{Sn}(\text{NR}_2)_2$  ( $\text{R} = \text{Me}, \text{Et}, \text{Pr}, \text{SiMe}_3$ ) have been investigated. With  $\text{Sn}(\text{N}^i\text{Pr}_2)_2$  and  $\text{Sn}(\text{NTMS}_2)_2$ , the anticipated products of amine elimination, iminophenoxy tin(II) mono(amide)s, are formed. However, for  $\text{R} = \text{Me}$  and  $\text{R} = \text{Et}$ , nucleophilic attack of the amide at the imino carbon occurs to generate tin(II) complexes of tetradentate, dianionic aminoamidophenoxide ligands. The transfer of the amide is shown to be reversible, with both alcoholysis and the initiation of *rac*-lactide polymerization apparently mediated by the terminal amide tautomer.

## Introduction

The industrial preparation of poly(lactic acid), PLA, from plant starch epitomizes the current interest in using renewable rather than depleting chemical feedstocks.<sup>1</sup> PLA is manufactured via the ring-opening polymerization of lactide, LA, using a poorly defined initiating species comprising tin(II) bis(2-ethylhexanoate) and alcohol. In order to produce single-site analogues of this system, tin(II) alkoxide and amide complexes of both  $\beta$ -diketiminates<sup>2</sup> and amidinate<sup>3</sup> ligand families have been reported by ourselves and Tolman et al. Despite deploying a wide range of ancillary ligand substituents, however, all of these initiators polymerize *rac*-LA with a similar level of heteroselectivity ( $P_r = 0.62$ – $0.65$ ), an observation attributed to the nonbonding nature of the tin  $5s^2$  electrons: poor spatial overlap with the  $4d$  and  $5p$  orbitals (due to a relativistic contraction) means that the tin center uses orthogonally aligned  $p$  and  $d$  orbitals for coordination

purposes, a constraint which almost entirely eliminates the influence of the ancillary ligand over the stereochemistry of the ring-opening event.<sup>2b</sup>

Stereochemical invariance at single-site catalytic centers is unusual, so we decided to explore the divalent tin chemistry of different monoanionic ancillary ligand systems. Salicylaldimines ( $\alpha$ -iminophenoxides) are one of the most commonly studied ligand classes in contemporary coordination chemistry, and their ease of synthesis makes them particularly attractive subjects for catalytic studies. The opportunity to realize enhanced polymerization activity and microstructural control by varying their steric and electronic properties has already been exploited in early<sup>4</sup> and late<sup>5</sup> transition (and even main group<sup>6</sup>) metal initiators for the polymerization of ethylene and higher  $\alpha$ -olefins.

Although their use as ligands for other monomer systems is somewhat less advanced, some salicylaldimine-based initiators have been reported for the ring-opening polymer-

\* E-mail: v.gibson@imperial.ac.uk (V.C.G.); e.marshall@imperial.ac.uk (E.L.M.).

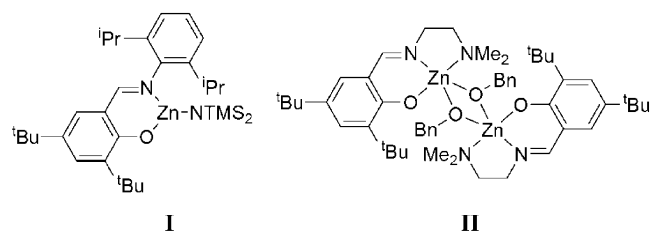
<sup>†</sup> Imperial College London.

<sup>‡</sup> Loughborough University.

- (1) Drumright, R. E.; Gruber, P. R.; Henton, D. E. *Adv. Mater.* **2000**, *12*, 1841–1846.
- (2) (a) Dove, A. P.; Gibson, V. C.; Marshall, E. L.; White, A. J. P.; Williams, D. J. *Chem. Commun.* **2001**, 283–284. (b) Dove, A. P.; Gibson, V. C.; Marshall, E. L.; Rzepa, H. S.; White, A. J. P.; Williams, D. J. *J. Am. Chem. Soc.* **2006**, *128*, 9834–9843.
- (3) (a) Aubrecht, K. B.; Hillmyer, M. A.; Tolman, W. B. *Macromolecules* **2002**, *35*, 644–650. (b) Nimitsiriwat, N.; Gibson, V. C.; Marshall, E. L.; White, A. J. P.; Dale, S. H.; Elsegood, M. R. J. *Dalton Trans.*, DOI 10.1039/b706663e.

- (4) (a) Mitani, M.; Mohri, J.; Yoshida, Y.; Saito, J.; Ishii, S.; Tsuru, K.; Matsui, S.; Furuyama, R.; Nakano, T.; Tanaka, H.; Kojoh, S.; Matsugi, T.; Kashiwa, N.; Fujita, T. *J. Am. Chem. Soc.* **2002**, *124*, 3327–3336. and references therein. (b) Tian, J.; Coates, G. W. *Angew. Chem., Int. Ed.* **2000**, *39*, 3626–3629. (c) Tian, J.; Hustad, P. D.; Coates, G. W. *J. Am. Chem. Soc.* **2001**, *123*, 5134–5135. (d) Hustad, P. D.; Tian, J.; Coates, G. W. *J. Am. Chem. Soc.* **2002**, *124*, 3614–3621. (e) Coates, G. W.; Hustad, P. D.; Reinartz, S. *Angew. Chem., Int. Ed.* **2002**, *41*, 2236–2257. (f) Gibson, V. C.; Mastroianni, S.; Newton, C.; Redshaw, C.; Solan, G. A.; White, A. J. P.; Williams, D. J. *J. Chem. Soc., Dalton Trans.* **2000**, 1969–1971. (g) Jones, D. J.; Gibson, V. C.; Green, S. M.; Maddox, P. J. *Chem. Commun.* **2002**, 1038–1039.
- (5) Younkin, T. R.; Connor, E. F.; Henderson, J. I.; Friedrich, S. K.; Grubbs, R. H.; Bansleben, D. A. *Science* **2000**, *287*, 460–462.

Scheme 1



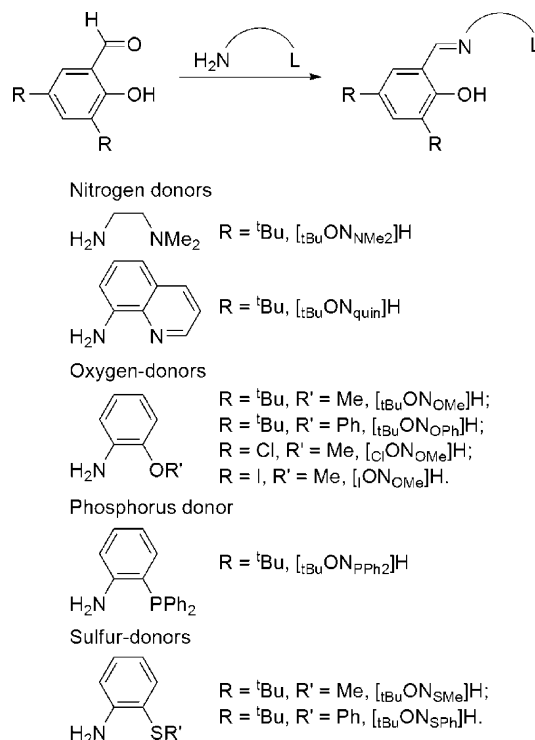
ization of lactide, most notably with Zn,<sup>7</sup> Mg,<sup>7c</sup> and Ca.<sup>8</sup> A clear message to arise from these studies is the difficulty in obtaining single-site behavior if the salicylaldimine binds merely as a bidentate chelate. For example, Chisholm and co-workers have successfully employed bidentate phenoxymimines to support three-coordinate zinc-based initiators, but single-site behavior requires both the Schiff base and the initiating nucleophile (either an aryloxy or amide) to be bulky (e.g., **I**, Scheme 1): slow consumption of L-LA ensues, with 20 equiv polymerized over 3 h at 25 °C.<sup>7a</sup> Lin et al. have shown that dimeric complexes of tridentate variants are more readily accessible, and less bulky counterparts of **II** (lacking the phenoxy *tert*-butyl substituents) afford much more active initiators than **I**, capable of consuming 200 equiv of LA in <30 min at room temperature.<sup>7b</sup>

In light of these results, we chose to investigate the tin(II) complexation chemistry of potentially tridentate salicylaldimines, with a view to producing single-site LA polymerization initiators. We were particularly interested to discover whether the presence of a third donor site might help overcome the influence of the 5s<sup>2</sup> electrons, leading to different PLA tacticities. As described below, this study instead led to the discovery of a rather unusual ligand amination reaction, aspects of which have been communicated.<sup>9</sup>

## Synthetic Studies

Salicylaldimines with a neutral donor atom bound to the imine functionality are readily obtained from the condensation of a 2,4-disubstituted salicylaldehyde with an appropriately functionalized amine or aniline (Scheme 2),<sup>10</sup> for the sake of brevity, these are abbreviated to [R<sub>2</sub>ON<sub>R'</sub>]H, where R represents the *ortho*- and *para*-phenol substituents, and R' indicates the N-substituent. These were chosen to allow a probe of both steric and electronic factors, particularly with respect to the imino donor arm, which features a range of N-, P-, O-, and S-based donor groups. The effects of

Scheme 2. Syntheses of Potentially Tridentate Salicylaldimines



halogenated substituents on the phenoxy ring have also been examined within the O-donor family.

Single-site initiators for the ring-opening polymerization of cyclic esters are typically alkoxide (–OR) complexes, although other nucleophilic ligands such as amides (–NR<sub>2</sub>) may also be used.<sup>11</sup> In order to prepare [R<sub>2</sub>ON<sub>L</sub>]Sn(OR) alkoxide complexes, a two-step route successfully used to synthesize β-diketiminato tin(II) analogues<sup>2</sup> was initially envisaged, that is, formation of [R<sub>2</sub>ON<sub>L</sub>]SnCl and subsequent metathesis with an alkali metal alkoxide. Thus, lithiation of [*t*BuON<sub>NMe<sub>2</sub></sub>]H, [*t*BuON<sub>PPh<sub>2</sub></sub>]H, [*t*BuON<sub>OMe</sub>]H, and [*t*BuON<sub>SPh</sub>]H with <sup>*n*</sup>BuLi, followed by addition to a suspension of SnCl<sub>2</sub> in toluene at room temperature, afforded the salicylaldimine tin(II) chloride complexes **1–4** in recrystallized yields of 74, 76, 49, and 64%, respectively (Scheme 3).<sup>10</sup>

However, all reactions of the chloride complexes with LiO<sup>*i*</sup>Pr and NaO<sup>*i*</sup>Bu led to intractable mixtures, with the exception of the reaction of **4** with NaO<sup>*i*</sup>Bu, for which recrystallization of the crude product mixture resulted in the isolation of the bischelate [*t*BuON<sub>SPh</sub>]<sub>2</sub>Sn, **5**. This synthetic route was therefore abandoned in favor of direct metalation with Sn(NMe<sub>2</sub>)<sub>2</sub>.<sup>12</sup> Due to high solubilities, the products arising from the reactions with [*t*BuON<sub>NMe<sub>2</sub></sub>]H, [*t*BuON<sub>OPh</sub>]H, and [*t*BuON<sub>SMe</sub>]H could not be readily purified by either washing or recrystallization. Nonetheless, complexes **6–11**, formed from the treatment of Sn(NMe<sub>2</sub>)<sub>2</sub> with [*t*BuON<sub>quin</sub>]H,

(6) (a) Cameron, P. A.; Gibson, V. C.; Redshaw, C.; Segal, J. A.; Bruce, M. D.; White, A. J. P.; Williams, D. J. *Chem. Commun.* **1999**, 1883–1884. (b) Cameron, P. A.; Gibson, V. C.; Redshaw, C.; Segal, J. A.; White, A. J. P.; Williams, D. J. *Dalton Trans.* **2002**, 415–422. (c) Annunziata, L.; Pappalardo, D.; Tedesco, C.; Pellecchia, C. *Organometallics* **2005**, *24*, 1947–1952.

(7) (a) Chisholm, M. H.; Gallucci, J.; Zhen, H.; Huffman, J. C. *Inorg. Chem.* **2001**, *40*, 5051–5054. (b) Chen, H.-Y.; Tang, H.-Y.; Lin, C.-C. *Macromolecules* **2006**, *39*, 3745–3752. (c) Wu, J.-C.; Huang, B.-H.; Hsueh, M.-L.; Lai, S.-L.; Lin, C.-C. *Polymer* **2005**, *46*, 9784–9792.

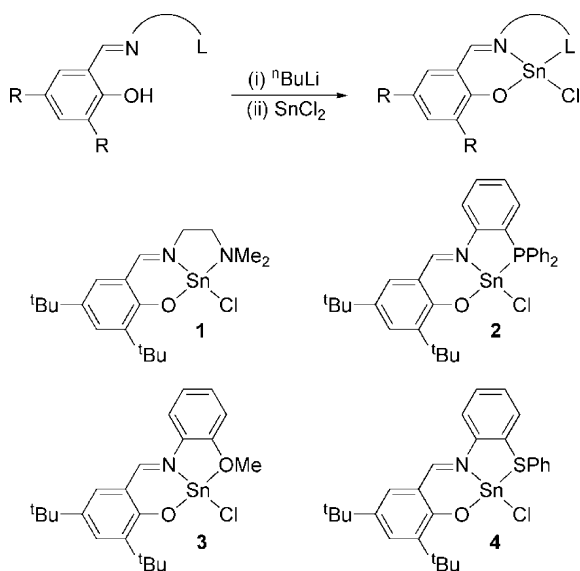
(8) Darendsbourg, D. J.; Choi, W.; Richers, C. P. *Macromolecules* **2007**, *40*, 3521–3523.

(9) Nimitsiriwat, N.; Marshall, E. L.; Gibson, V. C.; Elsegood, M. R. J.; Dale, S. H. *J. Am. Chem. Soc.* **2004**, *126*, 13598–13599.

(10) See Supporting Information.

(11) (a) O'Keefe, B. J.; Hillmyer, M. A.; Tolman, W. B. *Dalton Trans.* **2001**, 2215–2224. (b) Gibson, V. C.; Marshall, E. L. In *Comprehensive Coordination Chemistry II*; McCleverty, J. A., Meyer, T. J., Eds.; Elsevier: Oxford, 2003; Vol. 9, pp 1–74; (c) Nakano, K.; Kosaka, N.; Hiyama, T.; Nozaki, K. *Dalton Trans.* **2003**, 4039–4050. (d) Dechy-Cabaret, O.; Martin-Vaca, B.; Bourissou, D. *Chem. Rev.* **2004**, *104*, 6147–6176.

(12) Foley, P.; Zeldin, M. *Inorg. Chem.* **1975**, *14*, 2264–2267.

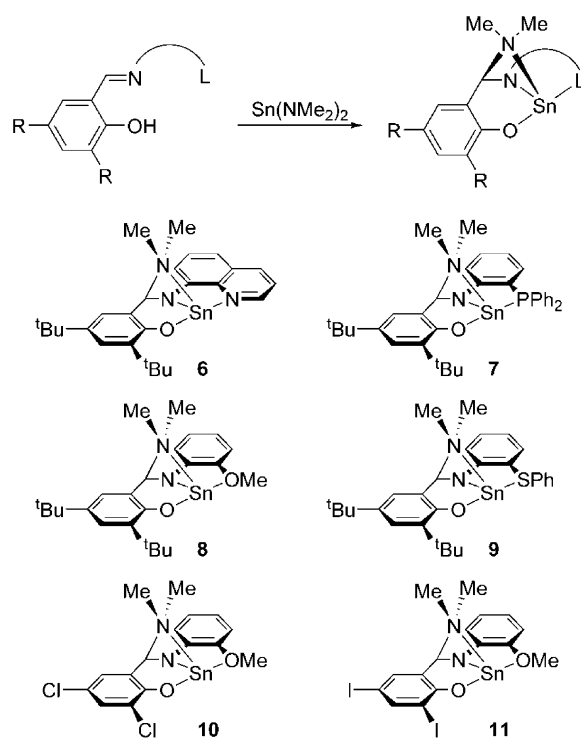
**Scheme 3.** The Syntheses of the Tin(II) Chloride Complexes **1–4**

$[\text{tBuONPPh}_2]\text{H}$ ,  $[\text{tBuONOMe}]\text{H}$ ,  $[\text{tBuONSPh}]\text{H}$ ,  $[\text{ClONOMe}]\text{H}$ , and  $[\text{IONOMe}]\text{H}$ , respectively, were isolated in analytically pure forms by recrystallization.

The  $^1\text{H}$  and  $^{13}\text{C}$  solution-state NMR spectra of the recrystallized samples of **6–11** share similar gross features but are all inconsistent with  $[\text{RON}_\text{L}]\text{Sn}(\text{NMe}_2)$  formulations. Most notably, no  $\text{HC}=\text{N}$  imino resonances are observed in the expected window of the  $^1\text{H}$  NMR spectra ( $\delta$  7.44–7.61 for **1–4**;  $\delta$  7.86 for **5**), although in every case a singlet, integrating as a solitary proton, is present between 5.35 and 5.70 ppm. The  $^{13}\text{C}$  NMR spectra all include a corresponding upfield-shifted resonance for the associated carbon atom (e.g., 87 ppm for **7** versus 169 ppm for **2**).  $^1\text{H}/^{13}\text{C}$  HMBC NMR experiments further indicated that in each of the six complexes the same carbon atom is separated from the  $\text{NMe}_2$  protons by just three bonds: a five-bond separation would be anticipated for  $[\text{RON}_\text{L}]\text{Sn}(\text{NMe}_2)$ .

X-ray diffraction studies on **7** and **11** revealed that both complexes contain tetradentate, dianionic ligands arising from amination of the imino  $\text{sp}^2$ -carbon atom. The  $\text{NMe}_2$  ligand becomes a neutral dative  $\sigma$ -donor to the metal, with the former imino N converted into an anionic amido ligand. As the NMR spectra of these two compounds are entirely representative of the family of **6–11**, the structures of **6** and **8–10** are therefore assigned by analogy, as summarized in Scheme 4.

In solution, the  $\text{Sn}-\text{NMe}_2$  interaction appears to be hemilabile, at least for complexes **6**, **8**, **10**, and **11**, all of which give one broad resonance for what should be inequivalent  $N$ -methyl protons; one broad signal is also observed for the  $\text{N}(\text{CH}_3)_2$  resonance in the  $^{13}\text{C}$  spectrum. Although one could interpret these data in terms of the reversible migration of the  $\text{NMe}_2$  unit from the tin to the imino carbon, sharp resonances for the  $\text{HCN}$  proton indicate that the broadening instead arises from the breaking and reforming of the dative  $\text{N}-\text{Sn}$  interaction. This is supported by low-temperature  $^1\text{H}$  NMR spectra in  $\text{CD}_2\text{Cl}_2$  which reveal that the  $\text{NMe}_2$  signals resolve into two sharp singlets.<sup>10</sup> A stronger interaction is apparently present at room temperature

**Scheme 4.** The Syntheses of the Bridged Amide Complexes **6–11**

in the diphenylphosphino-based **7**, the  $^1\text{H}$  and  $^{13}\text{C}$  NMR spectra of which contain two sharp singlets for the inequivalent  $\text{NMe}_2$  groups ( $\delta_\text{H}$  2.08 and 1.93;  $\delta_\text{C}$  43.80 and 40.87). A similar effect is observed in the phenylthioether-containing **9** ( $\delta_\text{H}$  1.94 and 1.80;  $\delta_\text{C}$  43.65 and 40.62). The reason why the  $\text{Sn}-\text{N}$  interaction appears stronger in these two compounds is not clear: one might anticipate that it would actually be weakest in these structures, with sterically bulky and relatively basic  $-\text{PPh}_2$  and  $-\text{SPh}$  substituents likely to result in congested metal centers of reduced electron deficiency. One explanation is that despite the presence of  $^{119}\text{Sn}-^{31}\text{P}$  coupling in the NMR spectra of **7** (see discussion of complex **15** below) the  $\text{Sn}-\text{P}$  and  $\text{Sn}-\text{S}$  interactions might be hemilabile in **7** and **9**, allowing stronger coordination of the amine (whereas the smaller  $\text{OMe}$  donors of **8**, **10**, and **11** are tightly bound to the tin center). Alternatively, the ring strain within the  $\text{SnN}_2\text{C}$  fragment may promote dissociation of the neutral amine donor: once this has occurred, the remainder of the ligand becomes free to maneuver into a less strained conformation, a process possibly disfavored for the heavier  $\text{PPh}_2$  and  $\text{SPh}$  units.

The molecular structure of **11** (Figure 1) shares many of the features previously described by us for complex **7**.<sup>9</sup> The phenoxy-based ligand is now tetradentate, with anionic amide  $[\text{Sn}(1)-\text{N}(1) = 2.111(3) \text{ \AA}]$  and coordinative dative amine  $[\text{Sn}(1)-\text{N}(2) = 2.404(3) \text{ \AA}]$  ligation [analogous bond lengths in **7** are 2.1649(12) and 2.4490(13)  $\text{\AA}$ ]. The removal of unsaturation from the former salicylaldehyde  $\text{C}=\text{N}$  functionality is confirmed by the similar  $\text{C}(8)-\text{N}(1)$  and  $\text{C}(8)-\text{N}(2)$  bond distances [1.448(5) and 1.503(4)  $\text{\AA}$  respectively]. The ethereal oxygen atom in **11** is displaced significantly further from the tin than its phenoxy counterpart ( $\text{Sn}-\text{O}(1) = 2.809(3) \text{ \AA}$ ;  $\text{Sn}-\text{O}(2) = 2.123(2) \text{ \AA}$ ), but this

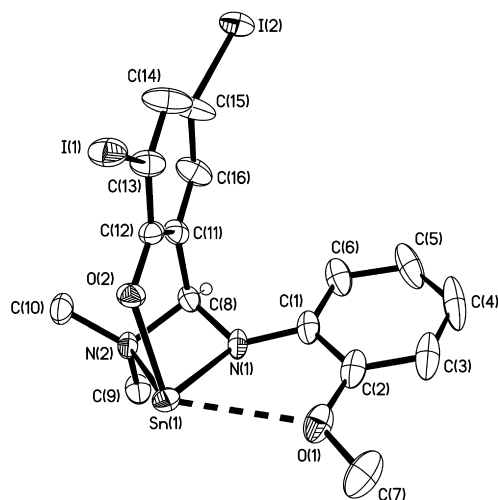


**Figure 1.** The molecular structure of complex **11**. Ellipsoids are at the 50% probability level. Selected bond lengths (Å) and bond angles (°): Sn(1)–N(1) = 2.111(3), Sn(1)–N(2) = 2.404(3), Sn(1)–O(2) = 2.123(2), Sn(1)–O(1) = 2.809(3), N(1)–C(8) = 1.448(5), N(2)–C(8) = 1.503(4); N(1)–Sn(1)–N(2) = 59.64(11), N(1)–Sn(1)–O(2) = 88.50(11), N(2)–Sn(1)–O(2) = 80.91(10); N(1)–C(8)–N(2) = 99.9(3), Sn(1)–N(1)–C(8) = 99.7(2), Sn(1)–N(2)–C(8) = 86.41(19), O(1)–Sn(1)–N(1) = 61.84(10), O(1)–Sn(1)–N(2) = 119.45(9), O(1)–Sn(1)–O(2) = 111.89(9).

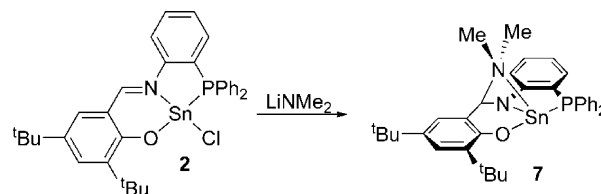
separation is still shorter than the sum of the respective van der Waals radii (2.17 Å (Sn) + 1.52 Å (O) = 3.69 Å<sup>13</sup>) and is comparable in length to another weak Sn–O interaction recently reported by us.<sup>2b</sup> Intermolecular approaches are shown in the Supporting Information, but none of these is of sufficient proximity to be considered a bonding interaction.<sup>10</sup>

The coordination sphere of the metal therefore contains a large region of seemingly unoccupied space. Previous computational studies<sup>2b</sup> suggest that for  $\beta$ -diketiminato counterparts the tin 5s orbital undergoes a relativistic contraction: assuming a similar situation exists here, the metal-based orbitals used to bind the tetradentate ligands will be orthogonally orientated 4d and 5p lobes: the presence in the crystal structure of **11** (and **7**) of several interligand angles at tin of ca. 90° (e.g., N(1)–Sn(1)–O(2) = 88.50(11); N(2)–Sn(1)–O(2) = 80.91(10); O(1)–Sn(1)–O(2) = 111.89(9)°) lends support to this hypothesis.

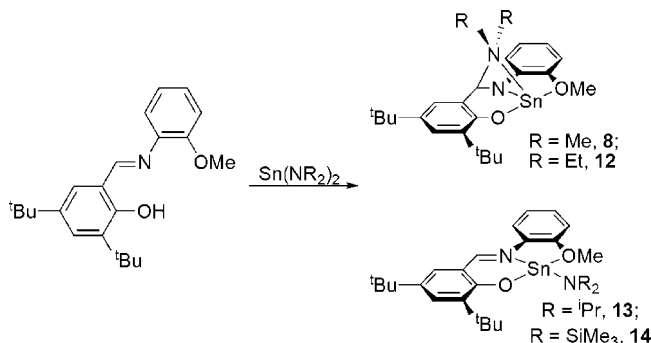
Two pathways are advanced to account for the formation of complexes **6–11**: one of the amide ligands of Sn(NMe<sub>2</sub>)<sub>2</sub> could attack the imino carbon atom prior to salicylaldehyde deprotonation, or the desired [R<sub>2</sub>ONL]SnNMe<sub>2</sub> species might form first and migration of the amide then occurs to complete the ligand transformation. The latter of these mechanisms appears more likely since the addition of LiNMe<sub>2</sub> to the chloride complex **2** also results in the clean formation of **7** (Scheme 5). <sup>1</sup>H NMR confirms that complexes **3** and **4** react similarly (though the products of these reactions were again too soluble to allow ready isolation of analytically pure products).

In order to further probe the versatility of the amination reaction, [tBuONMe]H was treated with Sn(NEt<sub>2</sub>)<sub>2</sub>, Sn(N<sup>i</sup>Pr)<sub>2</sub>, and Sn(NTMS)<sub>2</sub> to yield complexes **12–14**, respectively (Scheme 6), though **13** gradually decomposes in solution and has therefore only been characterized spectroscopically. <sup>1</sup>H

**Scheme 5.** Alternative Synthesis of Complex **7**



**Scheme 6.** The syntheses of complexes **8** and **12–14**



NMR spectra (Figure 2) confirmed that **12** possesses a similar ligand skeleton to that seen in **8** (e.g.,  $\delta$  CH(NEt<sub>2</sub>) = 5.79 cf.  $\delta$  CH(NMe<sub>2</sub>) = 5.44); by contrast, the spectra of **13** and **14** clearly demonstrate that ligand amination does not occur so readily with the bulkier tin(II) amides, with singlets characteristic of HC=N imine environments observed at 7.57 and 7.48 ppm, respectively, and no CH(NR<sub>2</sub>) resonances between  $\delta$  5 and 6. Similarly, the reaction of [tBuONPPh<sub>2</sub>]H with Sn[N(SiMe<sub>3</sub>)<sub>2</sub>]<sub>2</sub> cleanly afforded the terminal amide [tBuONPPh<sub>2</sub>]SnN(SiMe<sub>3</sub>)<sub>2</sub>, **15** ( $\delta$  HC=N = 7.15 ppm).

An X-ray crystallographic analysis of **15** confirms the terminal, monoanionic nature of the NTMS<sub>2</sub> amide ligand (Figure 3) and also reveals that in the solid state the salicylaldehyde ligand adopts a bidentate chelation mode. Unlike the Me<sub>2</sub>N-bridged complexes, the anilino ring is aligned in a near-orthogonal manner to the plane of the N(1)

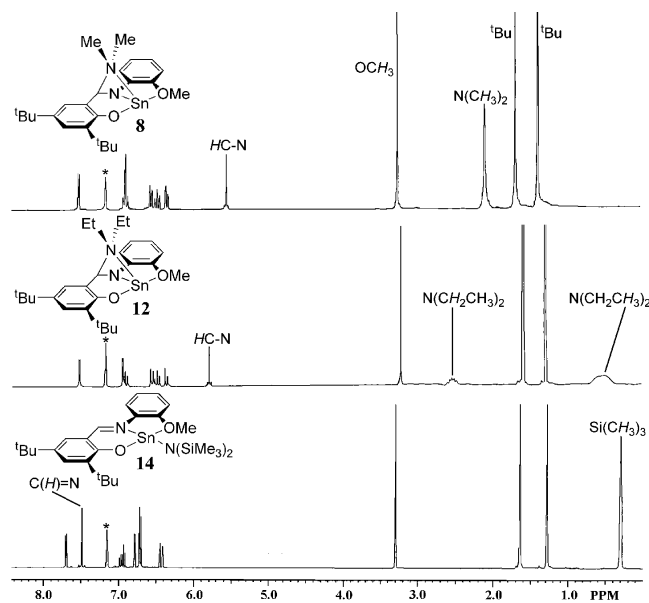


**Figure 2.** <sup>1</sup>H NMR spectra of complexes **8**, **12**, and **14** (C<sub>6</sub>D<sub>6</sub>, 250 MHz, 298 K; \* = C<sub>6</sub>D<sub>5</sub>H).

(13) Bondi, A. J. *Phys. Chem.* **1964**, *68*, 441–451.



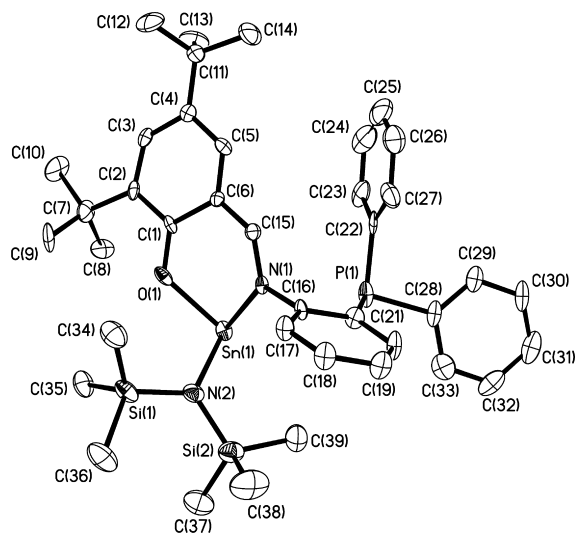


**Figure 3.** The molecular structure of complex **15**. Ellipsoids are at the 50% probability level. Selected bond lengths (Å) and bond angles (°): Sn(1)–N(1) = 2.328(7), Sn(1)–N(2) = 2.115(8), Sn(1)–O(1) = 2.112(6), N(1)–C(15) = 1.323(11), N(1)–C(16) = 1.425(11); N(1)–Sn(1)–N(2) = 92.6(3), N(1)–Sn(1)–O(1) = 79.9(2), N(2)–Sn(1)–O(1) = 96.4(3), C(1)–O(1)–Sn(1) = 124.7(5), C(15)–N(1)–Sn(1) = 119.6(6), Si(1)–N(2)–Si(2) = 123.5(5), Si(1)–N(2)–Sn(1) = 120.0(4), Si(2)–N(2)–Sn(1) = 114.2(4).

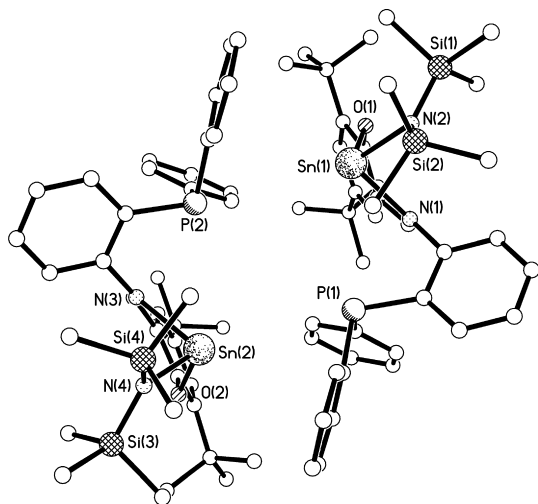


**Figure 4.** The asymmetric unit of complex **15**. Selected nonbonding distances (Å): Sn(1)···P(1) = 3.767, Sn(1)···P(2) = 4.126, Sn(2)···P(2) = 3.748, Sn(2)···P(1) = 4.089, Sn(1)–Sn(2) = 6.152.

substituents, placing the  $\text{PPh}_2$  moiety on the opposite side of the molecule to the  $\text{N}(\text{SiMe}_3)_2$  unit probably in order to minimize steric interaction between these two bulky groups. The Sn(1)···P(1) distance is 3.767 Å, and though slightly shorter than the sum of the van der Waals radii ( $2.17 (\text{Sn}) + 1.80 (\text{P}) = 3.97 \text{ Å}^{13}$ ) such a distance far exceeds the longest reported Sn–P bond [3.036(2) Å].<sup>14</sup>

Complex **15** crystallizes with two molecules in the asymmetric unit related by a noncrystallographic pseudo-2-fold rotation axis (Figure 4). There are no intermolecular interactions between the phosphorus and tin atoms, with both the Sn(1)–P(2) and Sn(2)–P(1) separations  $>4 \text{ Å}$ . The geometry of the tin center is therefore best described as a

trigonal pyramid, with the three-coordinate tin atom displaced by 1.109 Å from the O(1), N(1), N(2) plane. The Sn(1)–N(2) bond is approximately perpendicular to the O(1), Sn(1), N(1) plane [N(2)–Sn(1)–N(1) = 92.6(3), N(2)–Sn(1)–O(1) = 96.4(3)°]. The retention of the imine functionality is confirmed by the short C(15)–N(1) bond [1.323(11) Å] and the dative nature of the Sn(1)–N(1) interaction [2.328(7) Å, cf. Sn(1)–N(2) = 2.115(8) Å].

Despite the crystallographic data obtained on **15**, we believe that in solution the salicylaldimine ligands in complexes **14** and **15** probably coordinate in a hemilabile tridentate manner. Their  $^{119}\text{Sn}$  chemical shifts ( $\delta -150$  and  $-151$ , respectively) are downfield to some of the related four-coordinate bridged amine species (e.g.,  $\delta -166$ , **8**;  $-172$ , **12**;  $-271$ , **7**) but are not shifted sufficiently to indicate purely tricoordinate tin centers.<sup>15</sup> Tellingly, the  $^{31}\text{P}$  NMR spectrum of **15** consists of a singlet at  $-15.60 \text{ ppm}$  with satellites showing coupling to  $^{117}\text{Sn}$  and  $^{119}\text{Sn}$  (450 and 470 Hz, respectively); its  $^{119}\text{Sn}$  spectrum is a doublet at  $\delta -151$  with  $J_{\text{SnP}} = 460 \text{ Hz}$ . When compared to the analogous spectra of complex **7** ( $^{31}\text{P}$  NMR: singlet resonance  $\delta -16.38$ , unresolved satellites with  $J_{\text{SnP}} \approx 540 \text{ Hz}$ ;  $^{119}\text{Sn}$  NMR: doublet resonance  $\delta -271$ ,  $J_{\text{SnP}} = 538 \text{ Hz}$ ), it would appear that phosphorus coordination in solution is only slightly weaker in **15**.

In order to probe whether the amide migration is a reversible process, 10 equiv of  $\text{Me}_2\text{NH}$  was added to a solution of **12** in benzene- $d_6$  at ambient temperature and monitored by  $^1\text{H}$  NMR spectroscopy (Figure 5a). Within a few hours, the broad resonances at  $\delta 2.57$  and  $0.72$  corresponding to the bridging diethylamine group were seen to disappear and  $\text{Et}_2\text{NH}$  was generated, along with clean formation of the  $\text{Me}_2\text{N}$ -bridged complex **8**. Conversely, addition of excess  $\text{Et}_2\text{NH}$  (12 equiv) to a solution of **8** led to an incomplete conversion to **12** (Figure 5b;  $[\mathbf{8}]/[\mathbf{12}] \approx 1.6:1$ ;  $K_{\text{eq}} = 0.021$ ); the tin(II) complex containing the smaller amide bridge therefore appears to be thermodynamically more stable. Although direct observation of the terminal amide isomer of either **8** or **12** has not proved possible, we believe that transamination most likely proceeds via these intermediates (Scheme 7), particularly as precedence exists for the exchange of organic amines with metal-bound monoanionic amide ligands.<sup>16</sup>

Typically, metal amides also undergo facile alcoholysis,<sup>17</sup> so we next examined whether the bridged amine complexes might function as alkoxide precursors via their terminal amide tautomers. As anticipated, complex **8** reacts cleanly with  $\text{Ph}_2\text{CMeCOH}$  to afford the terminal alkoxide  $[\text{tBuO-NOMe}]_2\text{Sn}(\text{OCMePh}_2)_2$ , **16** (Scheme 8). However, smaller alcohols such as  $i\text{PrOH}$  and  $t\text{BuOH}$  led to intractable product mixtures, although the absence of  $\text{HC(OR)NAr}$  methine

(14) Barney, A. A.; Heyduk, A. F.; Nocera, D. G. *Chem. Commun.* **1999**, 2379–2380.

(15) (a) Hani, R.; Geanangel, R. A. *Coord. Chem. Rev.* **1982**, *44*, 229–246. (b) Hahn, F. E.; Wittenbecher, L.; Le Van, D.; Zabula, A. V. *Inorg. Chem.* **2007**, *46*, 7662–7667.

(16) Duan, Z.; Naiini, A. A.; Lee, J.-H.; Verkade, J. G. *Inorg. Chem.* **1995**, *34*, 5477–5482.

(17) Chisholm, M. H.; Rothwell, I. P. In *Comprehensive Coordination Chemistry*; Wilkinson, G., Gillard, R. D., McCleverty, J. A., Eds.; Pergamon: Oxford, 1987; Vol. 2, pp 161–188.

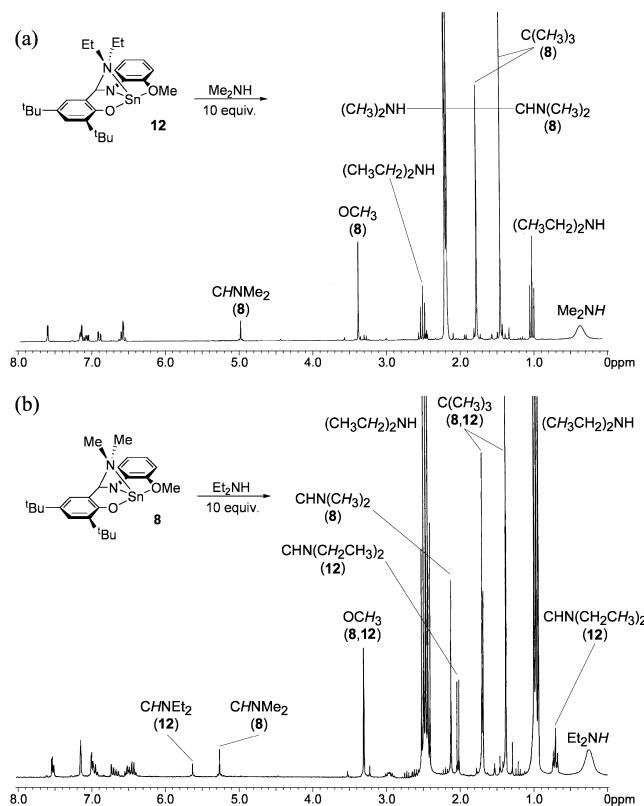
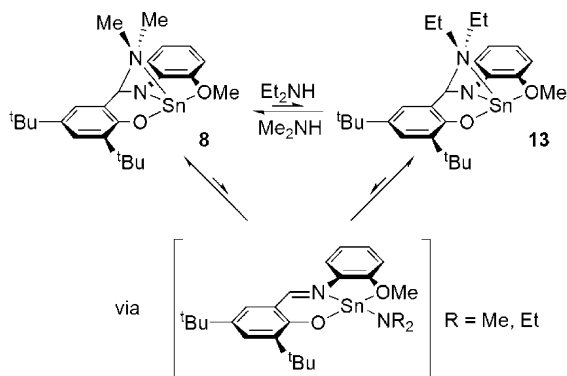
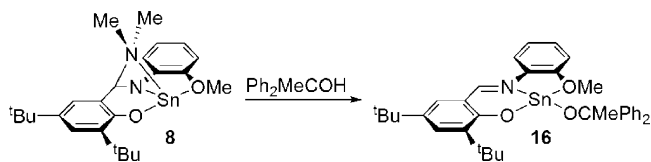


**Figure 5.**  $^1\text{H}$  NMR spectra ( $\text{C}_6\text{D}_6$ , 250 MHz, 298 K) of the reactions of (a) **12** +  $\text{Me}_2\text{NH}$  (10 equiv); (b) **8** +  $\text{Et}_2\text{NH}$  (10 equiv).

**Scheme 7.** Proposed Mechanism for the Amine Exchange Reactions



**Scheme 8.** The Synthesis of Complex **16** via Alcoholysis of **8**



NMR resonances (in both  $^1\text{H}$  and  $^{13}\text{C}$  spectra) indicates that a bridged ether ligand analogous to the bridged amine skeleton found in **6–11** is probably not present in the product mixture. Although the structure of **16** has not been established crystallographically, solution-state NMR data ( $\text{C}_6\text{D}_6$ ) are entirely consistent with the regeneration of the imino bond ( $\delta \text{HC}=\text{N}$  7.75;  $\delta \text{HC}=\text{N}$  166.44), and a  $^{119}\text{Sn}$  chemical shift of  $-379$  ppm points toward a four-coordinate metal center.

**Table 1.** Polymerization of *rac*-LA Using Initiators **6–11**<sup>a</sup>

	time (min)	conversion <sup>b</sup> (%)	induction period (min)	$k_{\text{app}}^c$ ( $\text{s}^{-1}$ )	$M_n^d$	$M_w/M_n^d$	$P_n^e$
<b>6</b>	360	91	74	$1.5 \times 10^{-4}$	19800	1.17	0.61
<b>7</b>	110	94	8	$4.7 \times 10^{-4}$	20500	1.25	0.60
<b>8</b>	120	91	7	$4.0 \times 10^{-4}$	18200	1.29	0.59
<b>9</b>	120	95	9	$4.4 \times 10^{-4}$	19100	1.27	0.59
<b>10</b>	60	92	<1	$7.4 \times 10^{-4}$	16000	1.57	0.65
<b>11</b>	100	95	0	$5.2 \times 10^{-4}$	23400	1.40	0.63

<sup>a</sup> All polymerizations were carried out at  $60^\circ\text{C}$  in toluene;  $[\text{LA}]/[\text{Sn}] = 100:1$ ;  $[\text{LA}] = 0.28 \text{ M}$ . <sup>b</sup> Determined by  $^1\text{H}$  NMR spectroscopy, integration of methine resonances of LA and PLA ( $\text{CDCl}_3$ , 250 MHz). <sup>c</sup>  $-d[\text{LA}]/dt = k_{\text{app}}[\text{LA}]$ , where  $k_{\text{app}} = k_p[\text{Sn}]^x$  ( $x$  = rate law order dependence on the initiator) —  $k_{\text{app}}$  values determined only after the induction period has elapsed. <sup>d</sup> Determined by gel permeation chromatography, calibrated with PS standards in  $\text{CHCl}_3$ . <sup>e</sup> Determined from the methine region of the homonuclear decoupled  $^1\text{H}$  NMR spectrum.

**Polymerization Studies**

The primary goal at the outset of this study was the synthesis of tin(II) alkoxide or amide complexes as single-site initiators for the ring-opening polymerization (ROP) of cyclic esters: the alkoxide **16** and terminal amide complexes **14** and **15** were therefore screened for *rac*-LA polymerization activity. Of these three, **16** is the most active, consuming 100 equiv of monomer in 240 min in toluene at  $60^\circ\text{C}$  (92% conversion;  $M_n = 21\,000$ ;  $M_n$  (calcd) = 13 300), but the molecular weight distribution is broader than expected for a well-behaved polymerization ( $M_w/M_n = 1.46$ ). The amide complexes are much less active, with 48 h at  $60^\circ\text{C}$  required to attain conversions of 64 and 93% for **14** and **15**, respectively. Furthermore, both initiators give very broad molecular weight distributions (**14**:  $M_n = 27\,400$ ;  $M_w/M_n = 6.1$ ; **15**:  $M_n = 20\,200$ ;  $M_w/M_n = 7.9$ ), consistent with several previous studies which describe inefficient initiation by bulky amide ligands.<sup>2b,18</sup>

Given that even the  $\text{OCMePh}_2$  ligand serves as a relatively poor initiating group, the use of smaller nucleophilic units was deemed preferable. Therefore, we next investigated whether the bridged  $\text{Me}_2\text{N}$  complexes **6–11** might function as polymerization initiators: it was envisaged that insertion of a lactide monomer into the  $\text{Sn}-\text{NMe}_2$  bond of the terminal amide  $[\text{R}(\text{ONL})\text{Sn}(\text{NMe}_2)]$  tautomers could lead to a terminal propagating species. As summarized in Table 1, all six examples are active with high conversions typically observed within just 2 h at  $60^\circ\text{C}$  and molecular weights close to predicted values ( $M_n$  (calcd) (PLA)<sub>100</sub> = 14 400).

The mode of action of **8** has been examined in detail by  $^1\text{H}$  NMR spectroscopy. The addition of 10 equiv of *rac*-LA to **8** in  $\text{C}_6\text{D}_6$  leads to the loss of the bridging amide group [ $\delta \text{HC}(\text{NMe}_2)$  5.55] and the regeneration of imino signals attributed to the propagating species:<sup>9</sup> all resonances are consistent with the presence at the metal center of a terminal propagating polyester group and a tridentate salicylaldiminato ligand. The  $^1\text{H}$  NMR spectra ( $\text{CDCl}_3$ ) of the PLA samples obtained from the polymerizations initiated by **6–11** also feature two singlet resonances ( $\delta$  2.94 and 3.03) attributable to the diastereotopic methyl groups of the  $\text{C}(\text{O})\text{NMe}_2$  chain

(18) Chamberlain, B. M.; Cheng, M.; Moore, D. R.; Ovitt, T. M.; Lobkovsky, E. B.; Coates, G. W. *J. Am. Chem. Soc.* **2001**, *123*, 3229–3238.

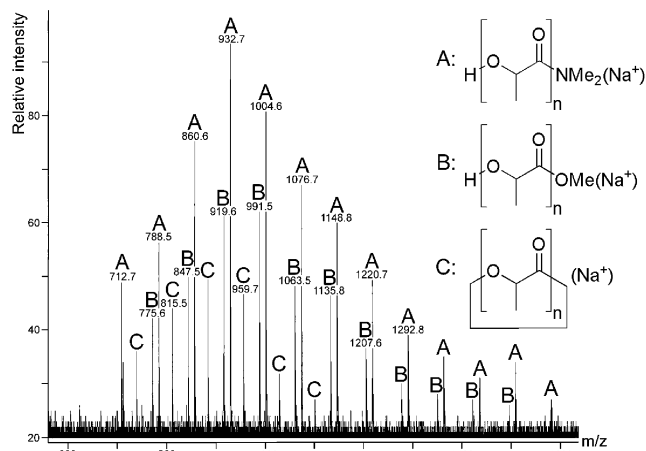


**Figure 6.** MALDI-TOF mass spectrum of PLA generated from initiator **8** ( $[LA]_0/[8] = 20$ , toluene, 60 °C, terminated with MeOH; matrix = 2,5-dihydroxybenzoic acid).

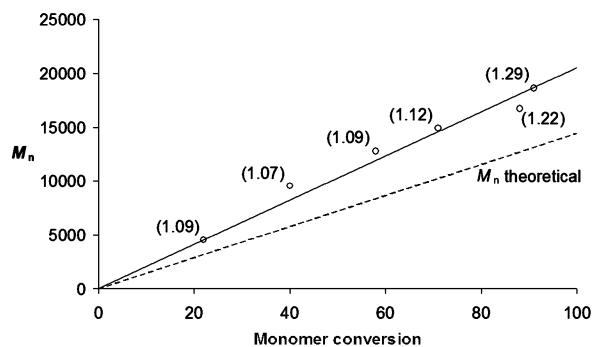


**Figure 7.** A plot of monomer conversion (%) versus  $M_n$  and correlation with theoretical  $M_n$  for the polymerization of *rac*-LA using **8** as an initiator ( $[LA]_0/[8] = 100$ , toluene, 60 °C; polydispersities shown in parentheses).

end group.<sup>10</sup> Furthermore, a MALDI-TOF mass spectrum of a sample of PLA prepared using **8** and 20 equiv of *rac*-LA confirms the presence of  $NMe_2$ -terminated chains (Figure 6, series **A**). Two other distributions,  $H-[O-C(H)CH_3-CO]_n-OMe$ ,  $Na^+$  (**B**) and cyclic PLA,  $Na^+$  (**C**) are observed: the latter is consistent with intramolecular transesterification,<sup>19</sup> whereas **B** might originate either from intermolecular transesterification of propagating chains by  $[Sn]-OMe$  species generated when the polymerization was terminated with excess MeOH or by partial acylation of the amide termini of **A** with methanol.<sup>20</sup>

These six initiators all give rise to well-controlled chain growth, with linear correlations between monomer conversion and  $M_n$  (exemplified in Figure 7 for **8**). The gradual rise in polydispersity values as the conversion increases reflects the increased prevalence for transesterification of the propagating chain as the concentration of monomer decreases. The notably broader distribution of chain lengths observed at high conversions with initiators **10** and **11** are also consistent with heightened levels of chain backbiting with more Lewis acidic active sites.<sup>2b</sup>

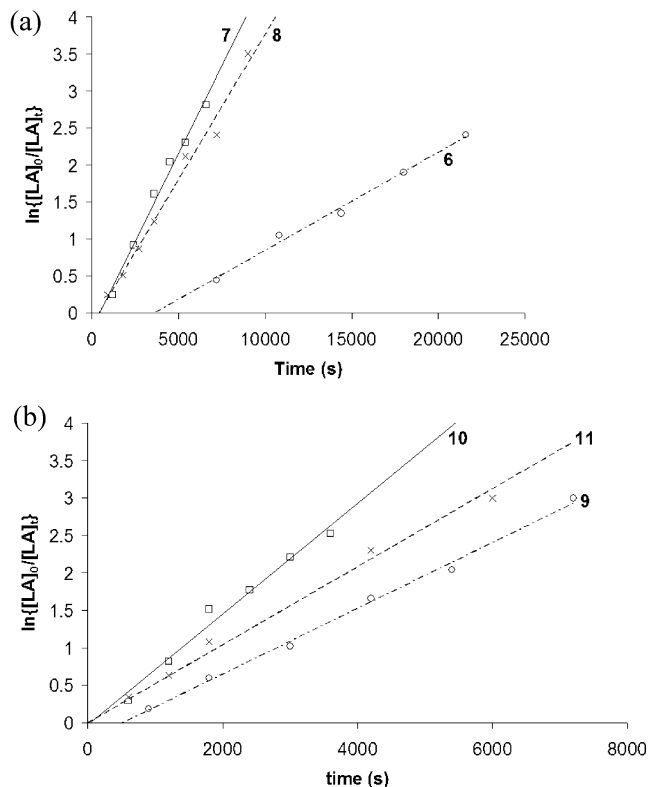


**Figure 8.** Plots of  $\ln\{[LA]_0/[LA]_t\}$  versus time (s) for: (a) complexes **6**, **7**, and **8**; (b) complexes **9**, **10**, and **11** ( $[LA]_0/[Sn] = 100$ , toluene, 60 °C).

The polymerizations initiated by complexes **6–11** all exhibit a first-order dependence upon the concentration of *rac*-LA (Figure 8) and, with the exception of the quinolyl-functionalized **6**, all attain >90% monomer conversion within 2 h, despite the variation in the ligand pendant arms. Nonetheless, some electronic effects may be delineated: for example, the diiodophenoxy-based **11** affords faster polymerization than its *tert*-butyl analogue **8**, in accord with its more Lewis acidic metal center.<sup>2b</sup> The chloro-substituted **10** is even more active, achieving high conversion in just 60 min. The particularly slow nature of **6** most likely results from the rigid nature of the quinolyl donor group obstructing the interconversion of at least one pair of stationary points along the insertion reaction coordinate.<sup>21</sup>

A more detailed kinetic study has been performed on initiator **7**. The relationship between  $k_{app}$  and  $[7]$  (Figure S3) is nonlinear,<sup>10</sup> and this indicates a non-first-order dependence on the initiator ( $-d[LA]/dt = k_{app}[LA]$ , where  $k_{app} = k_p[Sn]^x$  and  $k_p$  = rate of propagation).<sup>22</sup> As shown in Figure 9, however, the plot of  $\ln k_{app}$  versus  $\ln[7]$  is linear, and its gradient indicates a dependence upon the initiator of 0.57, that is,  $-d[LA]/dt = k_p[LA][7]^{0.57}$ . The activity of the tin(II) centers is therefore apparently tempered by aggregation, an effect also observed in amidinate tin(II) systems.<sup>3,23</sup> We have attempted to investigate the nature and degree of aggregation

(19) Montaudo, G.; Montaudo, M. S.; Puglisi, C.; Samperi, F.; Spassky, N.; LeBorgne, A.; Wisniewski, M. *Macromolecules* **1996**, *29*, 6461–6465.

(20) Nishiura, M.; Hou, Z.; Koizumi, T.; Imamoto, T.; Wakatsuki, Y. *Macromolecules* **1999**, *32*, 8245–8251. We wish to thank one of the reviewers for highlighting this possibility.

(21) Marshall, E. L.; Gibson, V. C.; Rzepa, H. S. *J. Am. Chem. Soc.* **2005**, *127*, 6048–6049.

(22) Williams, C. K.; Breyfogle, L. E.; Choi, S. K.; Nam, W., Jr.; Hillmyer, M. A.; Tolman, W. B. *J. Am. Chem. Soc.* **2003**, *125*, 11350–11359.

(23) Aubrecht, K. B.; Hillmyer, M. A.; Tolman, W. B. *Macromolecules* **2002**, *35*, 644–650.

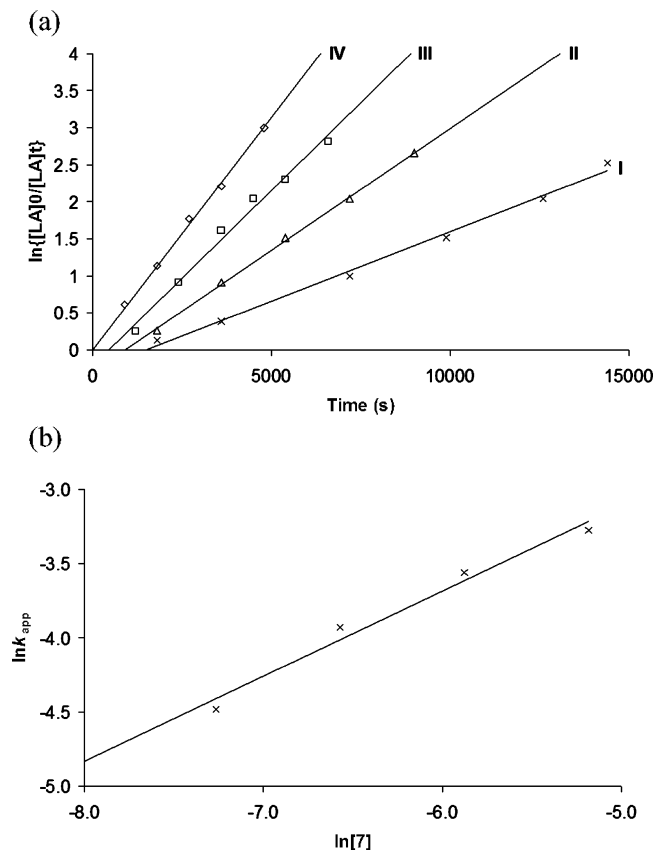


**Figure 9.** (a) Plots of  $\ln\{[LA]_0/[LA]_t\}$  versus time for the polymerization of *rac*-LA using 7 as the initiator ( $[LA] = 0.28 \text{ mol L}^{-1}$ ,  $[7] = 0.0007$  (I), 0.0014 (II), 0.0028 (III), 0.0056 (IV)  $\text{mol L}^{-1}$ , 60 °C, toluene); (b) a plot of  $\ln k_{app}$  versus  $\ln[7]$  for the polymerization of *rac*-LA using 7 as the initiator (60 °C, toluene).

further using cryoscopic measurements; unfortunately, to date, these have proved inconclusive.

All but the most active (i.e., 10 and 11) of these initiators display induction periods, though these are relatively short (<10 min) with the exception of 6 for which a delay of ca. 74 min exists before significant levels of propagation occur. Although the delay could arise from the formation of the active, terminal NMe<sub>2</sub> initiators, we believe a more likely explanation is that recently proposed for  $\beta$ -diketiminato tin(II) complexes<sup>2b</sup> and salen-supported titanium(IV) initiators;<sup>24</sup> that is, rapid formation of a particularly stable first insertion product is followed by much slower insertion of a second repeat unit with subsequent insertions gradually becoming more exothermic as dispersion forces associated with the propagating polymer increase with chain length.

Despite the variation in the ancillary ligand substituents, the microstructures of the PLA materials generated using 6–11 show little divergence from a moderate heterotactic

bias ( $P_r = 0.62 \pm 0.03$ ); this observation mirrors our findings with analogous  $\beta$ -diketiminato<sup>2</sup> and amidinate<sup>3,23</sup> tin(II) initiator families.

## Discussion

Although the metal complexation chemistry of salicylaldiminato ligands has been extensively studied, this is, to the best of our knowledge, the first observation of amide migration to the imine carbon. Although we have not been able to unambiguously explain why it should happen in this system, we believe that the divalent nature of the tin center is key. The solid-state structures obtained during this and related<sup>2,3</sup> studies indicate that the 5s orbital is reluctant to hybridize with the 4d or 5p orbitals, and the ligand donor atoms therefore occupy approximately orthogonally displaced coordination sites. This results in the proximal arrangement of the NMe<sub>2</sub> ligand and the electrophilic imino carbon, and this presumably lowers the barrier to the migratory process.

The amination reaction is reversible as shown by the exchange reactions of 8 with Et<sub>2</sub>NH and of 12 with Me<sub>2</sub>NH, and there is a clear preference for the bridging amide structure to incorporate smaller amide substituents. This observation most likely reflects steric crowding in the transition state associated with migration and in the resultant tetradentate ligand. Indeed, with the bulkier amide ligands N<sup>i</sup>Pr<sub>2</sub> and N(SiMe<sub>3</sub>)<sub>2</sub> amide transfer is hindered to such an extent that the terminal amide isomers 12–15 can be isolated. Furthermore, their isolation may be facilitated by potential hemilability of the salicylaldiminato ligands, as suggested by the bidentate coordination observed in the molecular structure of 15.

Although the precise mechanism for the amination reaction can not yet be stated with complete certainty, the intermediacy of terminal amide isomers is consistent with all the results obtained. For example, the reaction of alcohol with 8 can be likened to the enol-mediated reactivity of carbonyls; though present in low concentration, the terminal amide tautomer undergoes rapid alcoholysis and the tin(II)-containing equilibrium shifts accordingly. Similarly, the molecular weight control observed when these complexes are used to polymerize *rac*-lactide indicates that initiation via the terminal amide is rapid and quantitative.

**Acknowledgment.** The Royal Thai Government is thanked for a studentship (to N.N.).

**Supporting Information Available:** Full experimental details for the synthesis of complexes 1–16; .cif formatted files containing crystallographic data for complexes 11 and 15; crystallographic refinement details. This material is available free of charge via the Internet at <http://pubs.acs.org>.

IC701671S

(24) Gregson, C. K. A.; Blackmore, I. J.; Gibson, V. C.; Long, N. J.; Marshall, E. L.; White, A. J. P. *Dalton Trans.* **2006**, 3134–3140.